

This document is downloaded from DR-NTU, Nanyang Technological University Library, Singapore.

Title	Micromagnetic modeling of magnetic anisotropy in textured thin-film media
Author(s)	Zhao, Yang; Bertram, H. Neal
Citation	Zhao, Y., & Bertram, H. N. (1995). Micromagnetic modeling of magnetic anisotropy in textured thin film media. <i>Journal of applied physics</i> 77(12), 6411-6415.
Date	1995
URL	<a href="http://hdl.handle.net/10220/6734">http://hdl.handle.net/10220/6734</a>
Rights	©1995 AIP. This paper was published in <i>Journal of Applied Physics</i> and is made available as an electronic reprint (preprint) with permission of American Institute of Physics. The paper can be found at: [Doi: <a href="http://dx.doi.org/10.1063/1.359114">http://dx.doi.org/10.1063/1.359114</a> ]. One print or electronic copy may be made for personal use only. Systematic or multiple reproduction, distribution to multiple locations via electronic or other means, duplication of any material in this paper for a fee or for commercial purposes, or modification of the content of the paper is prohibited and is subject to penalties under law.

# Micromagnetic modeling of magnetic anisotropy in textured thin-film media

Yang Zhao and H. Neal Bertram<sup>a)</sup>

Center for Magnetic Recording Research, University of California at San Diego, La Jolla, California 92093

(Received 15 August 1994; accepted for publication 17 February 1995)

Existing micromagnetic models, based on single domain grains that individually follow coherent rotation during reversal, have been utilized to study the effect of various texture-induced microstructures on the hysteretic behavior of Co-alloy thin films with circumferentially textured substrates. The roles of preferential orientation of Co *c* axes, grain elongation, and segregation, as well as possible short-range intergranular coupling, have been examined in an effort to understand the origins of widely observed magnetic anisotropy in these media. Preferential *c*-axis distribution along the track direction yields reasonable remanences and coercivities for both circumferential and radial loops, but the observed loop closure remains unaccounted for by *c*-axis distribution alone. Closely packed arrays of elongated grains maintain relative isotropy in terms of magnetostatic interactions, while voids along texture lines contribute to the magnetostatic anisotropy of the film. The limitations of the model are also discussed. © 1995 American Institute of Physics.

## I. INTRODUCTION

In an effort to reduce head-medium stiction and friction, and to overcome the two-cycle modulation in read-back signal induced by in-line sputtering, commercial Co-alloy thin-film disk substrates are often given circumferential texture. Orientation ratio (OR), defined as the ratio of the remanence in the circumferential direction to that in the radial direction, and other magnetic properties such as coercivity, are found to have reduced fluctuations along the circumferential direction in these disks as compared to nontextured films.<sup>1-3</sup> Texturing of the substrate also gives rise to OR>1, the origin of which, though far from being sufficiently clarified, has received much experimental attention.<sup>1,3-9</sup> Suggestions have been made that preferential nucleation and growth of grains along texture lines result in OR>1.<sup>1,5,6</sup> In addition, it is speculated that crystallographic preferred orientation of the Cr underlayer is requisite to the formation of OR>1 on textured substrates for thin films of CoPtCr.<sup>4</sup> There are also reports of the presence of film discontinuities at the grooves corresponding to substrate textures in CoNi films with a Cr underlayer,<sup>3</sup> suggesting possible magnetostatic anisotropy in these films. Other studies have proposed magnetostrictive effects due to the in-plane strain induced by the textured substrate and composition of the magnetic layer.<sup>7,8</sup> Experimental studies have also been carried out to quantitatively determine the distribution of Co *c* axes of textured CoCr films,<sup>9</sup> showing that there is a greater population of crystals with their *c* axes pointing along the texture grooves. See also the recent work by Ishikawa *et al.*<sup>10</sup>

The purpose of this study is to examine theoretically the effect of various microscopic parameters, such as crystalline easy axis distribution, texture-induced grain elongations and separations, as well as intergranular coupling, on the hysteresis behavior of films. The micromagnetic model employed here is similar to that previously developed,<sup>11-14</sup> with the assumption of a monolayer of single domain grains interacting via magnetostatic and intergranular coupling. Features

such as OR, coercivities, and loop closures in tangential and radial directions are investigated for different texture-induced mechanisms.

## II. MICROMAGNETIC MODEL

Most practical thin films are composed of a polycrystalline Co alloy, deposited on a Cr underlayer, with crystallite size in the range of 10–50 nm. Grains of the magnetic layer are believed to be single domain, and are segregated by the Cr-rich intergranular phase for certain deposition conditions. The role of this phase in providing the magnetic coupling between neighboring grains is not entirely clear. Here, the simulation model assumes that single domain grains follow the Stoner–Wohlfarth coherent rotation mode during the reversal process. In most of the calculations, cells are hexagonal in shape and are placed on a 2D triangular lattice. The thickness of the film is set to be equal to the grain size. The effect of geometrical configurations on the magnetic anisotropy of the film is to be examined as a primary step of this study.

Energy density contributions include Zeeman energy due to a uniform external field, crystalline anisotropy energy, magnetostatic interactions, and intergranular coupling energy:

$$E_{\text{tot}} = E_{\text{ext}} + E_{\text{ani}} + E_{\text{mag}} + E_{\text{cpl}}. \quad (1)$$

The demagnetization energy of grain A due to source grain B is calculated by analytically integrating the field over eight surfaces of the source grain B, and then numerically averaging over volume of the grain A.<sup>12</sup> Self-demagnetization is treated in a similar fashion. The effective field on each grain is obtained from

$$\mathbf{H}_{\text{eff}} = - \frac{\partial E_{\text{tot}}}{\partial \mathbf{M}}. \quad (2)$$

The  $N$  ( $N$ =number of grains) coupled gyromagnetic equations of motion with Landau–Lifshitz damping are solved numerically with an adiabatically decreasing external field:

<sup>a)</sup>Electronic mail: nbertram@ucsd.edu

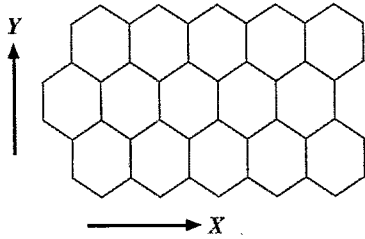


FIG. 1. Hexagonal grains placed on a planar triangular lattice. For most of the calculations, the X direction is chosen to be along the track direction.

$$\frac{d\mathbf{M}}{dt} = \gamma \mathbf{M} \times \mathbf{H}_{\text{eff}} - \frac{\lambda}{M} \mathbf{M} \times (\mathbf{M} \times \mathbf{H}_{\text{eff}}). \quad (3)$$

It is found that the precession term significantly increases computing time, while results are insensitive to the damping constant for large damping. The first term, which represents the gyromagnetic rotation, is therefore neglected. Periodic boundary conditions are employed in the calculation for arrays of grains with sizes varying from  $16 \times 16$  to  $64 \times 64$ . Vectorized 3D FFT codes are utilized to decrease the time of demagnetization field calculations, which are normally one of the most time-consuming parts of micromagnetic simulations.

### III. RESULTS AND DISCUSSION

#### A. Effect of hexagonal lattice structure

A triangular lattice has different symmetries in two orthogonal directions. For instance, the X direction in Fig. 1 is aligned with the grain boundaries while the same is not true for the Y direction. Furthermore, comparing the saturated state in the X direction and that in the Y direction, six nearest neighbors of a specific grain play different roles in providing magnetostatic interactions to the center grain, although the total sum of these interactions on the center grain is identical in these two cases. Therefore it is interesting to see if this configurational anisotropy in the model would result in a calculated magnetic anisotropy of the film. With each grain assigned an in-plane randomly oriented crystalline anisotropy, hysteresis behavior of this monolayer of closed-packed hexagonal grains is simulated in both X and Y directions. Surprisingly, when intergranular coupling is not present, the loops calculated in two directions are virtually identical, as shown in Fig. 2. This remains true for small intergranular exchange coupling. As the exchange coupling is increased, the finite size of the array begins to affect the calculation, causing nonidentical loops in the two directions. This result is somewhat different from the simulation done by Miles and Middleton,<sup>13</sup> in which they found that remanence and coercivity in these two directions differ significantly for films with no exchange coupling. In many of the Co-based thin films sputtered on circumferentially textured substrate, alignment of grain boundaries with texture lines can be clearly identified.<sup>5</sup> Accordingly, the X direction in Fig. 1 is chosen to be along the track in most of the simulations here. The purpose of this section is to show that hysteresis calculated from

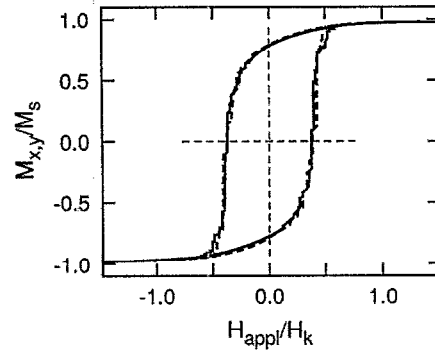


FIG. 2. Hysteresis loops for a monolayer of regular hexagonal grains in the absence of intergranular coupling ( $M_s/H_k=0.2$ ): solid, the X direction; dashed, the Y direction (see Fig. 1).

a hexagonal lattice does not contain a significant anisotropy, while the lattice itself contains an obvious threefold anisotropy. We do not attempt to prove that a grain pattern in which the grain boundaries are regularly aligned along one axis cannot show anisotropic hysteresis behavior.

#### B. Effect of crystallographic texture

It is well known that a Cr underlayer induces epitaxial growth of Co-alloy magnetic films with Co(11 $\bar{2}$ 0) planes parallel to Cr(001) planes. As Cr(001) planes tend to lie parallel to the local substrate surface, the Co *c* axes of films with a Cr underlayer are in the film plane. Thus a mostly in-plane orientation of *c* axes is expected for such films, and the distribution of *c* axes is planar isotropic if the substrate surface is untextured. However, when deposited on a circumferentially textured substrate, a greater population of grains are found to have their *c* axes directed along the grooves in CoCr films. In this paper, only textured thin films will be discussed. Other interesting media, such as bicrystal thin films,<sup>15,16</sup> are beyond the scope of this study.

A quantitative description has been proposed for the Co *c* axes distribution:<sup>19</sup>

$$f(\theta, \phi) = \frac{f_c(\phi)}{\sigma(\phi)} \exp\left[-\frac{(\pi/2 - \theta)^2}{2(\sigma(\phi))^2}\right], \quad (4)$$

where  $\theta$  and  $\phi$  follow the usual definition of polar coordinates with respect to the film normal (the *z* axis) and texture direction as the *x* axis, and

$$f_c(\phi) = \frac{f_{ip}}{(f_{ip}^2 \cos^2 \phi + \sin^2 \phi)^{1/2}}, \quad (5)$$

$$\sigma(\phi) = \sigma_0 \frac{f_{op}}{(f_{op}^2 \cos^2 \phi + \sin^2 \phi)^{1/2}}. \quad (6)$$

Measured parameters for the distribution are  $\sigma_0=0.039$ ,  $f_{ip}=0.40$ , and  $f_{op}=3.73$ . A plot of this distribution is given in Fig. 3. With the above *c*-axis distribution, hysteresis behavior has been simulated by assuming that the X direction in Fig. 1 is along the recording direction. Results are shown in Fig. 4. Similar circumferential and radial loops are found if the Y direction in Fig. 1 is taken as the circumferential

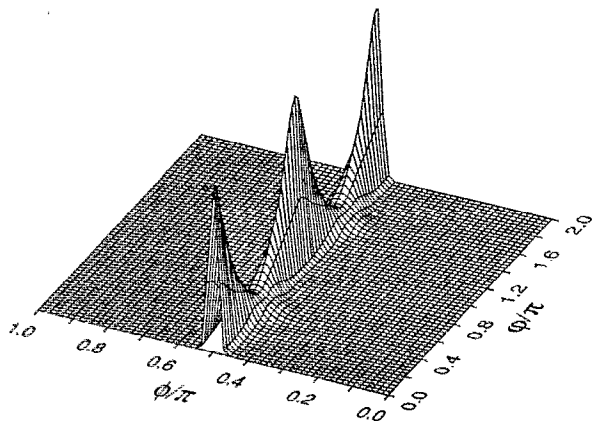


FIG. 3.  $c$ -axes distribution with  $\sigma_0=0.039$ ,  $f_{ip}=0.40$ , and  $f_{op}=3.73$ .

direction. The calculated loops give reasonable ratios of remanence and coercivity in circumferential and radial directions as compared to measurements.

It is often observed for disks with circumferentially textured substrates that the radial loop closes outside the circumferential one. This feature is missing in the simulated loops. Attempts have been made to numerically reproduce this feature by assuming a reasonable model of intergranular coupling based on either direct exchange coupling or a possible long-range RKKY interaction.<sup>17</sup> The latter introduces possible antiferromagnetic couplings between neighboring grains. None of the models have been successful in explaining the observed loop closure. An alternate model incorporating domain-wall pinning is proposed to understand texture-induced anisotropy in Ref. 18. In that model, the film is viewed as a continuous magnetic medium with different barriers (such as grain boundaries) that impede domain-wall motion. It is speculated that such a model might be necessary to explain the observed loop closure feature. We conclude that a distribution of Co  $c$  axes gives reasonable ratios of remanence and coercivity in two directions, but features such as loop closure are not well explained within the existing framework of the coherent rotation model.

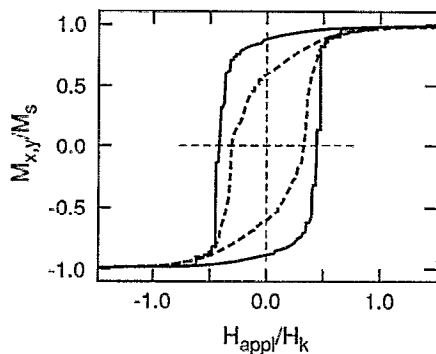


FIG. 4. Hysteresis loops for the  $c$ -axes distribution of Fig. 3: solid, circumferential direction; dashed, cross track direction. Other simulation parameters:  $M_s/H_k=0.2$ , no intergranular exchange coupling.

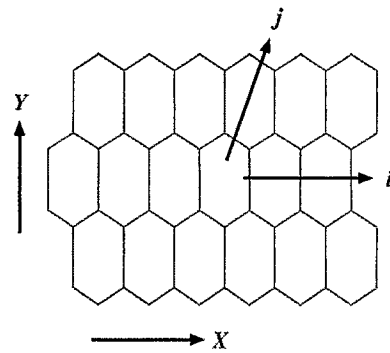


FIG. 5. Closely packed array of elongated grains

### C. Effect of grain elongation

For some thin-film disks with textured substrates, the geometry of Co-alloy grains was suggested by several investigators to have texture-induced acicularity.<sup>1,6</sup> Shape anisotropy has been viewed by many as one of the mechanisms responsible for  $OR > 1$ . Here, films with elongated grains are modeled by a closely packed array of elongated hexagons, as shown in Fig. 5. Elongation of grains is easily adjusted by varying  $D_y$  while fixing  $D_x$  to 1.0. The demagnetization matrix, which includes the self-demagnetization term or the shape anisotropy of the grain, is calculated similarly to that of regular hexagonal grains. Figure 6 compares the hysteresis loop in the direction of, and orthogonal to, grain elongation when  $D_y$  in Fig. 5 equals 1.4 ( $D_y$  equals 0.866 for a regular triangular lattice),  $M_s/H_k=0.2$ , and crystalline anisotropy is randomly oriented in the film plane. The close similarity between the two loops in Fig. 6 implies that films of closely packed single domain grains of elongated shape are relatively isotropic in terms of hysteresis behavior, regardless of the fact that grains are much elongated in one direction.

To better understand this point, the demagnetization matrix of the elongated structure is replaced by that of simple dipole-dipole interactions with dipoles positioned at geometrical grain centers. Simulations are then repeated for arrays of particles coupled by dipole-dipole interactions. Results are shown in Fig. 7. In contrast to Fig. 6, significant discrepancies are found between the hysteresis loops in these

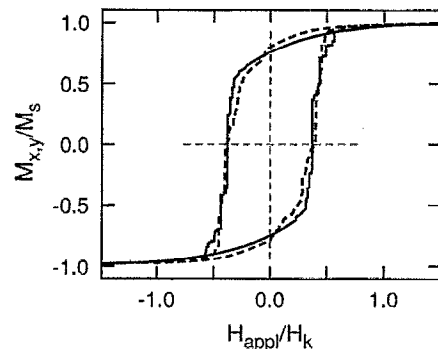


FIG. 6. Hysteresis loops for films of elongated grains: solid, the  $X$  direction; dashed, the  $Y$  direction (see Fig. 5).  $M_s/H_k=0.2$ , no intergranular coupling.

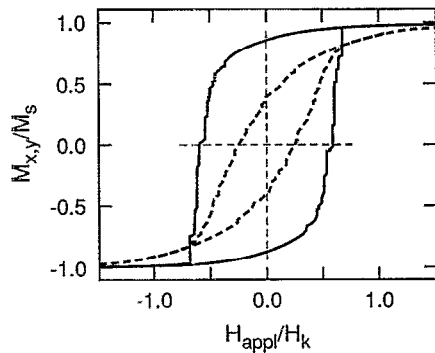


FIG. 7. Hysteresis loops for films in Fig. 5 if grains are coupled by simple dipole interactions ( $M_s/H_k=0.2$ ): solid, the X direction; dashed, the Y direction.

two directions. Coercivity and remanence in the Y direction are significantly lowered due to weakening of the magnetostatic coupling in that direction. Clearly, magnetostatic interactions of closely packed elongated grains bear no resemblance to the dipole-dipole form. In Fig. 8, the diagonal terms of the demagnetization matrix for an array of elongated grains, scaled by the corresponding terms of the dipole-dipole interactions for the same structure, are plotted in both  $\hat{i}$  and  $\hat{j}$  directions (see Fig. 5). For large  $i$  and  $j$ , the dipole-dipole form is expected to describe the magnetostatic interaction between well-separated grains, as demonstrated in Fig. 8. In the  $\hat{j}$  direction, where dipole-dipole interactions are much reduced by lattice elongation, the exact interactions exceed that of dipole-dipole form for small  $j$ , while the opposite is true in the  $\hat{i}$  direction when  $i$  is small. Since the shape anisotropy field in this case is merely  $1.3M_s$ , this buffering effect of magnetostatic interactions explains the relatively isotropic hysteresis. Further calculations indicate that as  $D_y$  is increased to 3.0, coercivities and remanences remain surprisingly close in the X and Y directions, although the loops begin to differ significantly.

#### D. Effect of film discontinuities along texture lines

Observations have shown that textures of the substrate generate gaps in thin films of Co-Ni/Cr.<sup>3</sup> To model film

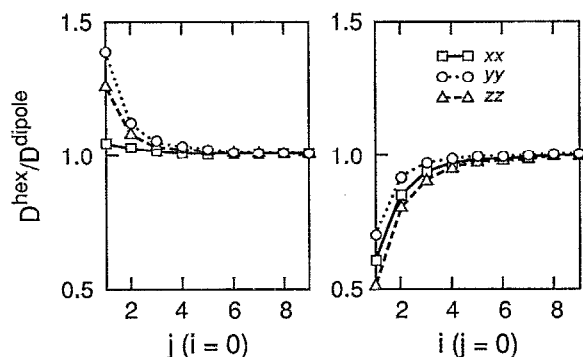


FIG. 8. The demagnetization matrix of film filled with elongated grains, scaled by point dipole interaction: (a)  $xx$ ,  $yy$ , and  $zz$  components along  $\hat{j}$  direction (see Fig. 5); (b)  $xx$ ,  $yy$ , and  $zz$  components along  $\hat{i}$  direction.

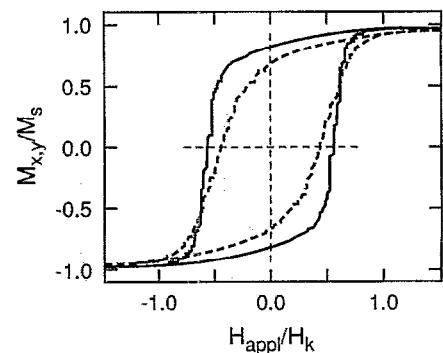


FIG. 9. Hysteresis loops for films with discontinuities along texture lines (anisotropy axes are randomly distributed in 2D): solid, along texture grooves; dashed, perpendicular to texture grooves.  $M_s/H_k=0.2$ , no intergranular coupling.

discontinuities at the grooves, which correspond to the texture lines on the substrate surface, an array of regular hexagonal grains is removed in the X direction (see Fig. 1) parallel to the track. The magnetizations of one out of every four rows of grains are set to zero in the micromagnetic calculation. Figure 9 shows the hysteresis loops of the X and Y directions when each grain is assigned a planar, randomly oriented  $c$  axis. Due to gap-induced anisotropy in the magnetostatic interaction, the radial loop actually closes outside the circumferential one. The loops shown in Fig. 9 are consistent with those in Fig. 7, where grains are coupled by dipole-dipole interaction, and the lattice is elongated in one direction. If a distribution of Co  $c$  axes of Eq. (4) is assumed for this gapped film, both remanence and coercivity increase for the circumferential loop and decrease for the radial loop, as shown in Fig. 10. Higher squareness of the circumferential loop can also be achieved by adding ferromagnetic intergranular coupling, instead of assuming a preferred orientation of  $c$  axes along the track direction, as demonstrated in Fig. 11. We observe that the inner loop ceases to close outside the outer loop due to the addition of ferromagnetic intergranular coupling.

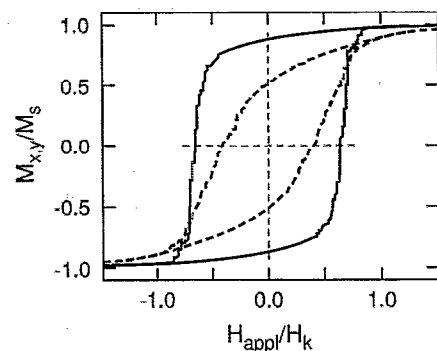


FIG. 10. Hysteresis loops for films with both a distribution of Co  $c$  axes and texture-induced discontinuities: solid, along texture grooves; dashed, perpendicular to texture grooves.  $M_s/H_k=0.2$ , no intergranular coupling.

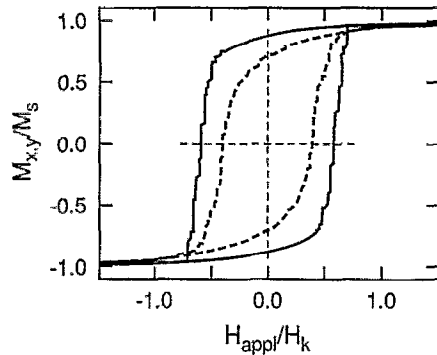


FIG. 11. Hysteresis loops for films with both texture-induced discontinuities and intergranular coupling: solid, along texture grooves; dashed, perpendicular to texture grooves.  $M_s/H_k=0.2$ ,  $H_{ex}/H_k=0.05$ .

#### IV. CONCLUSION

The impact of various texture-induced microstructures on the magnetic anisotropy of Co-alloy thin films has been examined within the framework of a micromagnetic model. Co  $c$ -axis distribution explains the observed disparity of coercivity and remanence in circumferential and radial directions, but detailed features such as the loop closure remain to be adequately explained. Magnetostatic interaction within closely packed arrays of elongated grains are found to be relatively isotropic. Identical coercivities and remanences are obtained in two orthogonal directions. Film discontinuities along texture lines may cause the radial loop to close outside the circumferential loop due to induced magnetostatic anisotropy. Further theoretical efforts are required to fully under-

stand the texture-induced anisotropy in Co-alloy disks and the reversal mechanisms of thin-film media at large.

#### ACKNOWLEDGMENTS

The authors would like to thank Professor B. M. Clemens for helpful discussions, and the San Diego Supercomputer Center for providing a grant to perform these computations. This research was supported by the National Science Foundation under Grant No. DMR-90-10908.

- <sup>1</sup>E. Teng and N. Ballard, IEEE Trans. Magn. **MAG-22**, 579 (1986).
- <sup>2</sup>K. E. Johnson, J. Appl. Phys. **69**, 4932 (1991).
- <sup>3</sup>S. Uchinami, F. Beppu, S. Ito, N. Tokubuchi, K. Noda, Y. Notohara, and K. Kanai, IEEE Trans. Magn. **MAG-23**, 3408 (1987).
- <sup>4</sup>M. Mizumaani, K. Johnson, D. Edmonson, P. Ivett, and M. Russak, J. Appl. Phys. **67**, 4695 (1990).
- <sup>5</sup>T. Lin, R. Alani, and D. N. Lambeth, J. Magn. Magn. Mater. **78**, 213 (1989).
- <sup>6</sup>E. M. Simpson, P. B. Narayan, G. T. K. Swami, and J. L. Chao, IEEE Trans. Magn. **MAG-23**, 3405 (1987).
- <sup>7</sup>R. Nishikawa, T. Hikosaka, K. Igarashi, and M. Kanamaru, IEEE Trans. Magn. **MAG-25**, 3890 (1989).
- <sup>8</sup>A. Kamamoto and F. Hikami, J. Appl. Phys. **69**, 5151 (1991).
- <sup>9</sup>H. Kataoka, J. A. Bain, S. Brennan, and B. M. Clemens, J. Appl. Phys. **73**, 7591 (1993).
- <sup>10</sup>A. Ishikawa, T. Ohno, S. Sakano, and Y. Shiroishi, J. Magn. Magn. Mater. **120**, 357 (1993).
- <sup>11</sup>G. F. Hughes, J. Appl. Phys. **54**, 5306 (1983).
- <sup>12</sup>J. Zhu and H. N. Bertram, J. Appl. Phys. **68**, 3248 (1988).
- <sup>13</sup>J. J. Miles and B. K. Middleton, IEEE Trans. Magn. **MAG-26**, 2137 (1990).
- <sup>14</sup>R. C. Giles and M. Mansuripur, J. Appl. Phys. **69**, 4712 (1991).
- <sup>15</sup>M. Mirzamaani, C. V. Jahans, and M. A. Russak, J. Appl. Phys. **69**, 5169 (1991).
- <sup>16</sup>B. Y. Wong, D. E. Laughlin, and D. N. Lambeth, IEEE Trans. Magn. **27**, 4733 (1991).
- <sup>17</sup>D. C. Mattis, *The Theory of Magnetism I* (Springer, Berlin, 1981).
- <sup>18</sup>N. Koga, S. Ito, and H. Tomiyasu, IEEE Trans. J. Magn. Jpn. **4**, 680 (1989).